



Sodium-carbonate co-substituted hydroxyapatite ceramics

Zoltan Z. Zyman*, Mykola V. Tkachenko

Physics of Solids Department, V.N. Karazin Kharkiv National University, 4, Svoboda Sq., Kharkiv 61022, Ukraine

Received 9 September 2013; received in revised form 28 November 2013; accepted 8 December 2013

Abstract

Powders of sodium-carbonate co-substituted hydroxyapatite, having sodium content in the range of 0.25–1.5 wt.% with a 0.25 wt.% step, were prepared by a precipitation-solid state reaction route. Compacts of the powders were sintered in a CO_2 flow (4 mL/min) at 1100 °C for 2 h. The sintered ceramics contained sodium and carbonate ions in the ranges of 0–1.5 wt.% and 1.3–6 wt.%, respectively, which are typical impurity concentrations in biological apatite. A relationship between sodium and carbonate contents and the type of carbonate substitution was found. The total carbonate content progressively increased with the sodium content. The obtained ceramics showed an AB-type carbonate substitution. However, the substitution became more B-type as the sodium content increased. As a result, the carbonation was almost B-type (94 %) for the highest sodium content (1.5 wt.%).

Keywords: sodium-carbonate co-substituted hydroxyapatites, sintering, characterization

I. Introduction

Biological apatite based on hydroxyapatite, HA, has a number of substitutions in cationic and anionic sublattices. The substitutions significantly affect the chemical and physico-chemical properties of the apatite, like mineralization and demineralization processes of calcified tissues and susceptibility to caries of teeth. Sodium (Na^+) and carbonate (CO_3^{2-}) ions are some of the major substituents occurring at levels of *ca* 0.9 wt.% and 5–8 wt.% [1–4].

As nanosize of crystals and their separation from the organic matrix cause difficulties in the apatite examination, synthetic carbonated hydroxyapatites, CHAs, are typically used as structural models for studying the growth and dissolution processes of biological crystals. Such studies also result in the development of bioactive materials for medical purposes [5–13]. The effect of sodium substitution in HA has extensively been studied [14–18], however, the simultaneous sodium-carbonate substitutions have not been examined as often. Besides, only limited combinations of the sodium and carbonate concentrations have been reported [19–24].

The sodium and carbonate ions have been introduced into HA in various ways. These have been (i) precipitation, with addition of sodium and carbonate into the mother solution containing soluble salts [19,20]; (ii) wet precipitation combined with a preliminary mechanical activation of parent reactants [24] or with firing powder samples in a wet carbon dioxide atmosphere [23]; (iii) synthesis at a high temperature and moderate pressure [22].

A recent *in vivo* study revealed that sodium-free CHA enhanced bone in-growth and coverage [25]. However, an *in vitro* study of sodium-carbonate HA showed that the co-substitution brought little enhance in osteoblast proliferation or phenotype expression compared to HA [25,26]. The processing routes indicated above may result in different physico-chemical characteristics, structural perturbations and, particularly, in CO_3^{2-} distributions in the lattice (A-, AB-, and B-types of substitution [5,10]) of sodium-bearing CHAs designed as the same product. This may cause contradicting biological behaviour of such compounds.

In this study, a relationship between sodium and carbonate concentrations in a wide range in biological crystals, and modes of carbonate distribution for each designed combination of the substituents was found in substituted apatite ceramics prepared by a simple reliable route.

* Corresponding author: tel: +38 057 707 56 84,
e-mail: intercom@univer.kharkov.ua
mykola.v.tkachenko@univer.kharkov.ua, tkanick53@mail.ru

Table 1. Elemental analysis of the sodium-substituted carbonated ceramics

Sample notation	Na [wt.%]	Ca [wt.%]	PO ₄ [wt.%]	C [wt.%]	H [wt.%]
CHA-0	0	40.6	54.6	0.27	0.15
CHA-1	0.25	40.3	54.4	0.53	0.15
CHA-2	0.50	40.1	53.0	0.78	0.13
CHA-3	0.75	39.6	52.6	0.90	0.11
CHA-4	1.00	39.5	52.5	1.10	0.11
CHA-5	1.25	39.5	52.0	1.08	0.10
CHA-6	1.50	38.2	52.0	1.20	<0.1

II. Materials and methods

An initial powder of carbonated hydroxyapatite (CHA) was prepared through the reaction of calcium carbonate, CaCO₃, (Merck, Germany, analytical grade) and a solution of the phosphate acid, H₃PO₄, (Merck) [2,27]. Sodium dopants were introduced into the CHA powder by soaking the powder in a solution of sodium hydrocarbonate, NaHCO₃, at 60 °C until the solvent was completely evaporated. The concentration of solution was varied so that the amount of sodium in the ceramics resulted from firing of compacts of such soaked powders was from 0.25–1.5 wt.% with a step of 0.25 wt.%. The compacts in the form of pellets (3 mm height and 10 mm diameter) were prepared in a steel mold by uniaxial pressing under 120 MPa. The compacts were sintered in a muffle in a dry CO₂ flow (4 mL/min) at 1100 °C for 2 h. Six batches of sintered compacts were prepared with five samples of each sodium concentration.

Calcium and sodium amounts in the samples were determined by atomic absorption spectroscopy (Thermo Electron Corporation, M-series AA spectrometer). Corresponding amounts of orthophosphate were found by colorimetry using the molybdenum blue method (Varian Cary Win UV spectrophotometer, $\lambda = 725$ nm). Carbon and hydrogen contents were measured by the burning method (EA 1110 CHNS-0 elemental analyser). Structural analysis was performed using a Philips APDW 40C diffractometer and a copper K_α radiation ($\lambda = 0.154$ nm) with a nickel filter through 20–70° diffraction angles (2θ). IR spectra were recorded by employing a BIO-RAD 175 spectrometer at a 2 cm⁻¹ resolution and the KBr technique, operating in the transmittance mode between wave numbers of 400–4000 cm⁻¹.

Figure 1 shows XRD patterns of ceramics without sodium (CHA-0) and with 1.25 wt.% of sodium (CHA-5). The patterns are identical, indicating that the addition of sodium does not change the crystallographic structure of the apatite. The XRD patterns show several sharp peaks characteristic of the hexagonal apatite structure. The patterns are centered around 26, 28, 30, 32, and 34 degrees 2θ.

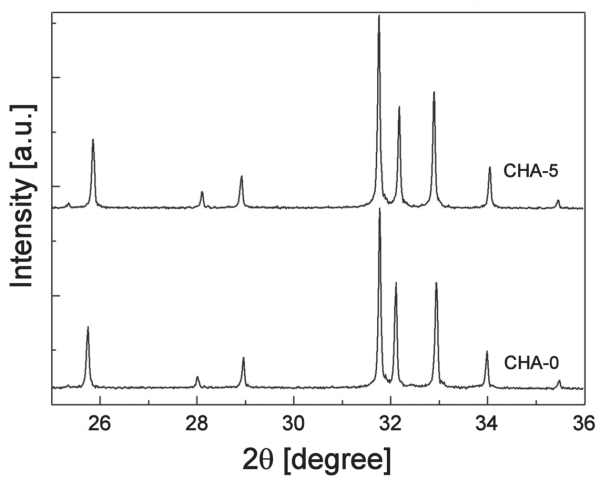


Figure 1. XRD patterns of ceramics without sodium (CHA-0) and with 1.25 wt.% of sodium (CHA-5)

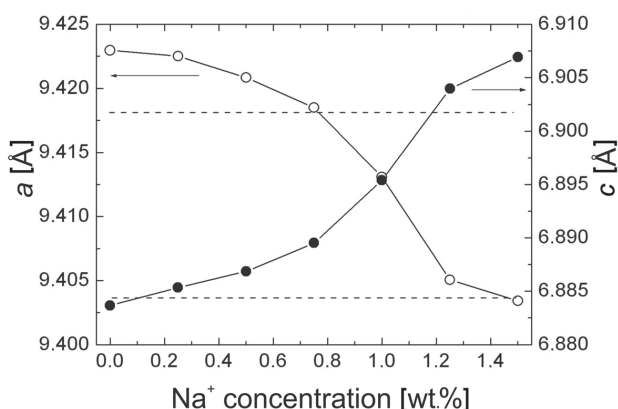


Figure 2. Lattice constants of ceramics with varying sodium concentration (the dotted horizontal lines are the reference values of HA)

III. Results and discussion

Compositions of the sintered ceramics, with given sodium concentrations, are listed in Table 1. The pivotal result is the interrelation between the sodium and carbon concentrations: the higher the value for sodium, the higher is the carbon content. The comparison of the XRD patterns for ceramics with no sodium and a high sodium content shows no changes in the crystallographic apatite structure (Fig. 1). However, the lattice constants substantially change (Fig. 2). Starting from the reference values of HA (the *a* constant is a little enhanced compared to the reference value because the ceramics was sintered in the CO₂ atmosphere [23,28]), the *a* constant gradually decreased, and the *c* constant gradually increased as the sodium content in-

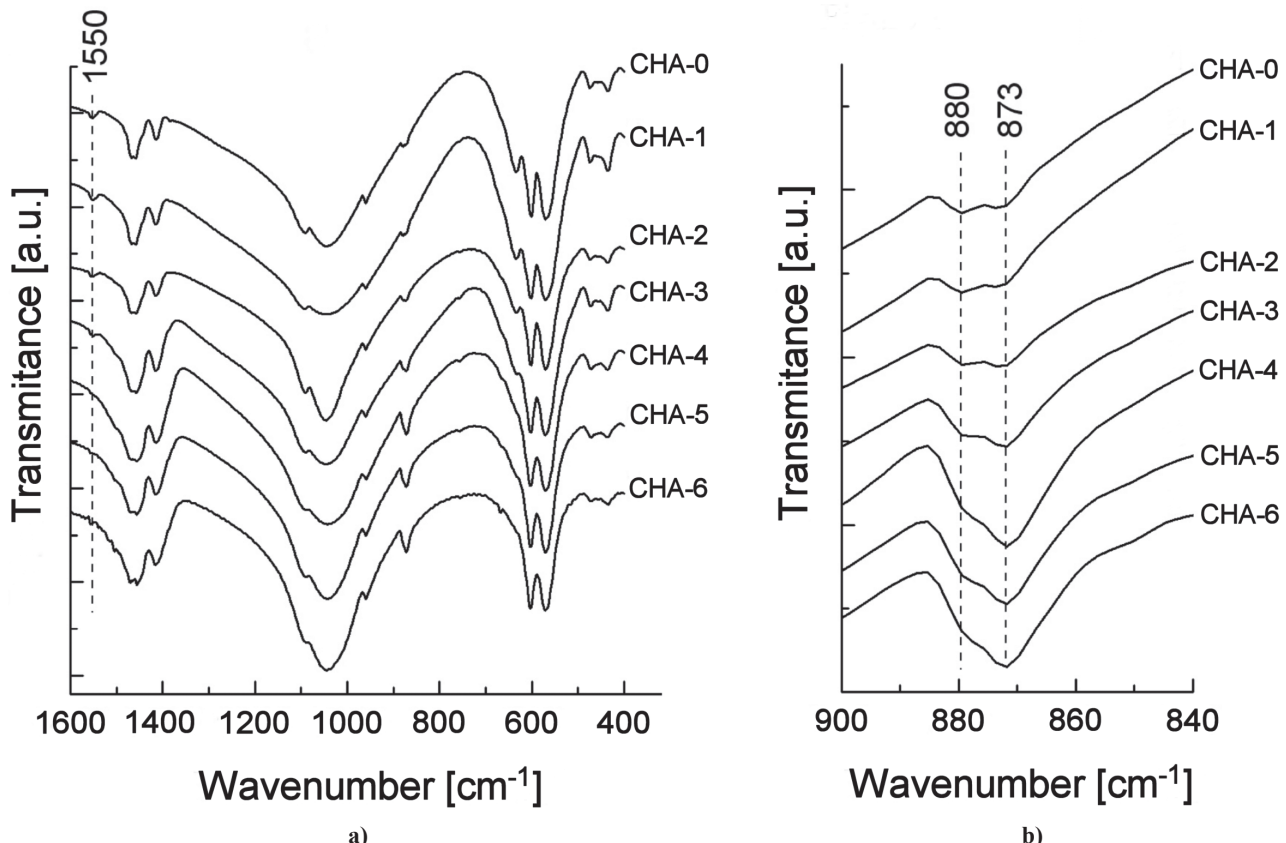


Figure 3. Fragments of IR spectra for ceramics with different sodium contents: 0 wt.% (CHA-0), 0.25 wt.% (CHA-1), 0.5 wt.% (CHA-2), 0.75 wt.% (CHA-3), 1.0 wt.% (CHA-4), 1.25 wt.% (CHA-5) and 1.5 wt.% (CHA-6)

creased in the ceramics. Most probably, this is not a result of the Na^+ for Ca^{2+} substitution as the effective ionic radii of Na^+ (0.99 Å) and Ca^{2+} (1.00 Å) are very close [29]. The change in lattice constants could be

caused by increased carbonate content in these ceramics (Table 1). However, the presence of carbonate may differently affect the lattice constants in CHA depending on the substitution site [5,10].

IR spectra of all sintered ceramics displayed typical absorbance bands of CHA (Fig. 3a): PO_4^{3-} bands at $478\text{ cm}^{-1}(\nu_2)$, 563 and $603\text{ cm}^{-1}(\nu_4)$, $965\text{ cm}^{-1}(\nu_1)$, 1055 , 1075 , 1085 and $1105\text{ cm}^{-1}(\nu_3)$; two resolved peaks or shoulders at about 634 and 3571 cm^{-1} of vibrational and stretching modes of OH^- , respectively; a broad vibrational band with a pick at about 3400 cm^{-1} and a sharp one at 1640 cm^{-1} of adsorbed water; clear peaks and more or less resolved shoulders at 1410 , 1450 , 1460 , 1475 , 1500 , 1515 cm^{-1} and, particularly, at 1545 and 1570 cm^{-1} in the $\nu_3\text{CO}_3^{2-}$ region and at about $875\text{ cm}^{-1}(\nu_3\text{CO}_3^{2-})$ indicated an AB-type CHA [10,13,22]. The sodium doping mainly affected the carbonate content in the CHAs. Fragments of IR spectra associated with CO_3^{2-} absorbance are depicted in Fig. 3. Comparative analysis of the spectra reveals that the prominent absorbance at 1550 cm^{-1} , associated with carbonates in A-positions, becomes weaker as the sodium content in the CHA increases (Fig. 3a). In the end, the absorbance disappears in spectra of ceramics with a sodium content above 1 wt.%. This is consistent with the decrease in hydrogen content (Table 1) and weakening of the OH^- band (at 634 cm^{-1}) in the spectra which may be attributed to the increasing occupation of A-site with carbonates as the sodium content increase. Analysis (decon-

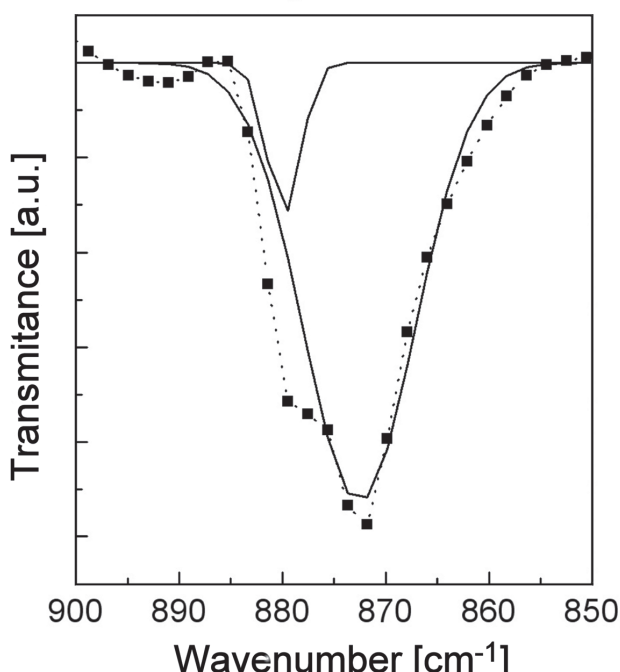


Figure 4. Deconvolution of the band at $\sim 875\text{ cm}^{-1}$ (sample CHA-3) performed using Gauss functions and the Fityk program

volution performed using Gauss functions and the Fityk program - an example is shown in Fig. 4) of the $\nu_2\text{CO}_3^{2-}$ domain sheds some light on this fact. Deconvolution of the band at about 875 cm⁻¹ for two peaks at 880 and 873 cm⁻¹ (Fig. 3b) associated with carbonates in A- and B-sites, respectively [10], reveals that, though decreasing in relative intensity as the sodium content increases, the band at 880 cm⁻¹ is present in each of the spectra, i.e. all sintered ceramics are CHA of an AB-type.

The areas under ν_3 and (or) $\nu_2\text{CO}_3^{2-}$ domains increased as the amount of sodium increased. This results from increasing carbonate content in the ceramics. The relative distribution of carbonates in the lattice was also evaluated. For this, the area of the $\nu_2\text{CO}_3^{2-}$ region was used because several bands in the $\nu_2\text{CO}_3^{2-}$ domain are associated with the both types of CO_3^{2-} . The baseline for the $\nu_2\text{CO}_3^{2-}$ range was determined as it was suggested earlier [30]. The total CO_3^{2-} concentration in each ceramics, represented by the area of $\nu_2\text{CO}_3^{2-}$ absorbance (the area approach fits better such a representation than the peak height way [31]), was calculated using the corresponding content of carbon (Table 1) and assuming that the latter entirely results from CO_3^{2-} . Using the whole area under the $\nu_2\text{CO}_3^{2-}$ range and the areas of the deconvoluted peaks (at 880 and 873 cm⁻¹) compiling this area, the distribution of the carbonates in A- and B-sites was calculated as the ratios of corresponding areas for each ceramics (Fig. 5). It can be seen that, as the content of the sodium substituent increases: i) the total carbonate amount also increases and ii) the amount and the accumulation rate of carbonate in B-sites are much higher than those in A-sites. These result in formation of almost B-carbonated ceramics for higher sodium concentrations (e.g. 94 % for 1.5 wt.% of Na^+ , Fig. 5). The increase in carbonation on B-site led to stronger corresponding absorbances and broadening (detected increase of the areas) of the ν_2 and $\nu_3\text{CO}_3^{2-}$ -regions (Fig. 3a). The overlap of the broadened B-carbonate absorbances in the ν_3 region with the band at 1550 cm⁻¹ gives a worse resolution in this region of the spectra. As a result, the band at 1550 cm⁻¹ gradually transforms to a shoulder and final-

ly disappears at above 1 wt.% of Na^+ (Fig. 3a) despite the presence and even slight increase of the carbonate content in A-sites (Fig. 5, curve 2).

The carbonate content in the sintered ceramics is in the range of 1.3–6.0 wt.% for sodium concentration in the range of 0–1.5 wt.%, respectively (Fig. 5). Such combinations of the sodium and carbonate co-substitution are characteristic of bone [2–4]. Thus, the prepared ceramics are supposed to manifest enhanced biological behaviour compared to unsubstituted calcium phosphates or only carbonated HA materials [25].

A reason of the transition of an A-B type apatite to a mainly B-type apatite with Na^+ -substitution observed in the study may be associated with lower defect formation energy of the later (−71 kJ/mol) compared to that of the former (−518.7 kJ/mol) [32] resulting in a more stable structure.

IV. Conclusions

1. Sodium-carbonate co-substituted HA ceramics were prepared through the introduction of sodium by a diffusion way into a nanocrystalline HA powder and sintering compacts of the sodium-doped powder in a CO_2 flow at high temperature. Ceramics with 0–1.5 wt.% sodium contained 1.3–6.0 wt.% carbonate, respectively. All ceramics were carbonated in both A- and B-sites.
2. The total carbonate concentration in ceramics increased progressively with the sodium content. A distribution of carbonates in A- and B-sites of the lattice for variety of sodium contents was obtained. The higher the sodium content, the higher was the carbonate concentration in B-sites compared to that in A-sites. As a result, about 94 % of the total carbonate in the lattice was accumulated in B-sites at 1.5 wt.% of sodium.
3. The combination of sodium and carbonate contents in the ceramics was within the typical values of natural bone, and so the ceramics can be considered as prospective biomaterials.

Acknowledgments: The authors are grateful to Prof. M. Epple (Duisburg-Essen University, Germany) for providing modern equipment for checking measurements.

References

1. F.C.M. Driessens, *Bioceramics of calcium phosphates*, CRC Press, Boca Raton, 1983.
2. T.S.B. Narasaraju, D.E. Phebe, “Some physico-chemical aspects of hydroxyapatite”, *J. Mater. Sci.*, **31** (1996) 1–21.
3. B.D. Ratner, *Biomaterials science: An introduction to materials in medicine*, Elsevier, Academic Press, 2004.
4. M. Epple, E. Bauelein, *Handbook of Biominerallisation: Medical and clinical aspects*, Wiley – VCH, Weinheim, 2007.

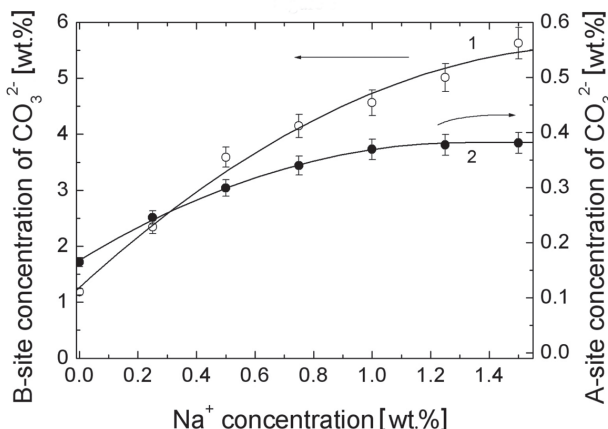


Figure 5. Distribution of carbonates in the A- and B-sites of the lattice in CHA ceramics doped with sodium

5. R.Z. LeGeros, O.R. Ttrauts, E. Klein, J.P. LeGeros, “Two types of carbonate substitution in the apatite structure”, *Experientia*, **25** (1969) 5–7.
6. D.G.A. Nelson, “The influence of carbonate on the atomic structure and reactivity of hydroxyapatite”, *J. Dent. Res.*, **60** (1981) 1621–1629.
7. L.G. Ellies, D.G.A. Nelson, J.D.B. Featherstone, “Crystallographic structure and surface morphology of sintered carbonated apatites”, *J. Biomed. Mater. Res.*, **22** (1988) 541–553.
8. Y. Doi, T. Koda, N. Wakamatsu, T. Goto, H. Kamemizu, Y. Moriwaki, M. Adachi, Y. Suwa, “Influence of carbonate on sintering of apatites”, *J. Dent. Res.*, **72** (1993) 1279–1284.
9. J.C. Merry, I.R. Gibson, S.M. Best, W. Bonfield, “Synthesis and characterization of carbonate hydroxyapatite”, *J. Mater. Sci.: Mater. Med.*, **9** (1998) 779–783.
10. I.R. Gibson, W. Bonfield, “Novel synthesis and characterization of an AB-type carbonate-substituted hydroxyapatite”, *J. Biomed. Mater. Res.*, **59** (2002) 697–708.
11. J.P. Lafon, E. Champion, D. Bernache-Assollant, R. Gibert, A.M. Danna, “Thermal decomposition of carbonated calcium phosphate apatites”, *J. Therm. Anal. Calorim.*, **72** (2003) 1127–1134.
12. E. Landi, A. Tampiery, G. Celotti, L. Vichi, M. Sandri, “Influence of synthesis and sintering parameters on the characteristics of carbonate apatite”, *Biomaterials*, **25** (2004) 1763–1770.
13. Z. Zyman, M. Tkachenko, “CO₂ gas-activated sintering of carbonated hydroxyapatites”, *J. Eur. Ceram. Soc.*, **31** (2011) 241–248.
14. I. Lopez-Valero, C. Gome-Lorente, R. Boistelle, “Effects of sodium and ammonium ions on occurrence, evolution and crystallinity of calcium phosphates”, *J. Cryst. Growth.*, **121** (1992) 297–304.
15. J.C. Elliot. *Structure and chemistry of the apatites and other calcium orthophosphates*, Elsevier, Amsterdam, 1994.
16. S. Kannan, J.H.G. Rocha, J.M.F. Ferreira, “Synthesis and thermal stability of sodium, magnesium co-substituted hydroxyapatites”, *J. Mater. Sci.*, **16** (2006) 286–291.
17. J. Ue, R.M. Pilliar, R.A. Kandel, “The effect of sodium dopants on calcium polyphosphate biomaterials”, *Key Eng. Mater.*, **361-363** (2008) 281–284.
18. K. Matsunaga, H. Murata, “Formation energies of substitutional sodium and potassium in hydroxyapatite”, *Mater. Trans.*, **50** (2009) 1041–1045.
19. H. El Feki, J.M. Savariault, A. Ben Salah, “Structure refinements by the Rietveld method of partially substituted hydroxyapatite: Ca₉Na_{0.5}(PO₄)_{4.5}(CO₃)_{1.5}(OH)₂”, *J. Alloys Compd.*, **287** (1999) 114–120.
20. H. El Feki, J.M. Savariault, A. Ben Salah, M. Jemal, “Sodium and carbonate distribution in substituted calcium hydroxyapatite”, *Solid State Sci.*, **2** (2000) 577–586.
21. R.M. Wilson, J.C. Elliot, S.E.P. Dowker, R.I. Smith, “Rietveld structure refinement of precipitated carbonate apatite using neutron diffraction data”, *Biomaterials*, **25** (2004) 2205–2213.
22. M.E. Fleet, X. Liu, “Coupled substitution of type A and B carbonate in sodium-bearing apatite”, *Biomaterials*, **28** (2007) 916–926.
23. J.A. Stephen, C. Pace, J.M.S. Skakle, I.R. Gibson, “Comparison of carbonate hydroxyapatite with and without sodium cosubstitution”, *Key Eng. Mater.*, **330-332** (2007) 19–22.
24. S.M. Barinov, I.V. Fadeeva, D. Ferro, J.V. Rau, S. Nunziante Cesaro, V.S. Komlev, A.S. Fomin, “Stabilization of carbonate hydroxyapatite by isomorphic substitutions of sodium for calcium”, *Russ. J. Inorg. Chem.*, **53** (2008) 164–168.
25. N. Patel, I.R. Gibson, K.A. Hing, S.M. Best, E. Damien, P.A. Revell, W. Bonfield, “The in vivo response of phase pure hydroxyapatite and carbonate substituted hydroxyapatite granules of varying size ranges”, *Key Eng. Mater.*, **218-220** (2002) 383–386.
26. K.A. Hing, J.C. Merry, I.R. Gibson, L. Di Silvio, S.M. Best, W. Bonfield, “Effect of carbonate content on the response of human osteoblast-like cells to carbonate substitute hydroxyapatite”, *Bioceramics*, **12** (1999) 185–188.
27. Z.Z. Zyman, M.V. Tkachenko, D.V. Polevodin, “Preparation and characterization of biphasic calcium phosphate ceramics of desired composition”, *J. Mater. Sci.: Mater. Med.*, **19** (2008) 2819–2825.
28. J.E. Barralet, G.J.P. Fleming, C. Campion, J.J. Harris, A.J. Wright, “Formation of translucent hydroxyapatite ceramics by sintering in carbon dioxide atmospheres”, *J. Mater. Sci.*, **38** (2003) 3979–3993.
29. R.D. Shannon, “Revised effective ionic radii and systematic studies of interatomic distances in halides and chalcogenides”, *Acta Cryst.*, **A32** (1976) 751–767.
30. A.B.S. Clasen, I.E. Ruyter, “Quantitative determination of type A and B carbonate in human deciduous and permanent enamel by means of Fourier transform infrared spectrometry”, *Adv. Dent. Res.*, **11** (1997) 523–527.
31. B.C. Smith, *Fundamentals of Fourier Transform Infrared Spectroscopy*, CRC Press, Boca Raton, 2011.
32. S. Peroos, Z. Du, N.H. de Leeuw, “A computer modelling study of the uptake, structure and distribution of carbonate defects in hydroxyapatite”, *Biomaterials*, **27** (2006) 2150–2161.

